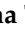




Article

Characterization of Alkali Activated Materials Prepared from Continuous Attrition and Ball Milled Fly Ashes

Jadambaa Temuujin ¹, Batmunkh Davaabal ², Ulambayar Rentsennorov ², Enkhtur Odbaatar ³, Dashnyam Enkhbayar ³, Tserendagva Tsend-Ayush ³, Sunjidmaa Danzandorj ⁴, Claus Henning Ruescher ^{5,*} and Kenneth J. D. MacKenzie ⁶

¹ School of Advanced Study, CITI University, Ulaanbaatar 14190, Mongolia; temuujin.jadamba@citi.edu.mn

² Institute of Chemistry and Chemical Technology, Mongolian Academy of Sciences, Ulaanbaatar 13330, Mongolia

³ Erdenet Minerals Institute, Erdenet Mining Corporation, Erdenet 61027, Mongolia

⁴ School of Architecture and Building, Mongolian University of Science and Technology, Ulaanbaatar 14191, Mongolia

⁵ Institute of Mineralogy, Leibniz University of Hannover, Callinstrasse 3, D-30167 Hannover, Germany

⁶ School of Chemical and Physical Sciences, Victoria University of Wellington, Wellington 6012, New Zealand

* Correspondence: c.ruescher@mineralogie.uni-hannover.de

Abstract: Mechanical activation is known to greatly influence the reactivity of fly ashes. In this paper, we report a comparative study of the properties of alkali-activated geopolymer materials prepared using both ball-milled and attrition-milled fly ashes. Ball milling was carried out for 30 min and 60 min while attrition milling was carried out continuously in a high-speed attritor. The surface area of the raw fly ash decreased from 4017 cm²/g to 3999 cm²/g and 3912 cm²/g after ball milling for 30 min and 60 min, respectively. By contrast, the surface area of the continuously attrition-milled fly ash increased to 5545 cm²/g. Fly ash processed by continuous attrition milling showed a 50% particle size reduction to 25–38 μm, whereas fly ash ball-milled for 30 and 60 min was reduced in size by 33.4 and 42.9%. The milled fly ash samples were activated with 8 M NaOH solution and cured at 40 °C for 68 h. After curing, the samples were maintained at room temperature, and their 7-, 14-, and 28-day compressive strengths were measured. The compressive strength of the attrition-milled 28-day geopolymer paste was 24.6 MPa; that of the geopolymers ball-milled for 30 and 60 min was 23.37 MPa and 17.58 MPa, respectively; and that of the unmilled control geopolymer fly-ash-based paste was 17 MPa. The improvement in the mechanical properties is attributed to the increased gel formation resulting from the increased surface area (decreased particle size) in the fly ash glass starting material.

Keywords: fly ash; continuous attrition milling; ball milling; microstructure; geopolymers



Citation: Temuujin, J.; Davaabal, B.; Rentsennorov, U.; Odbaatar, E.; Enkhbayar, D.; Tsend-Ayush, T.; Danzandorj, S.; Ruescher, C.H.; MacKenzie, K.J.D. Characterization of Alkali Activated Materials Prepared from Continuous Attrition and Ball Milled Fly Ashes. *Minerals* **2023**, *13*, 490. <https://doi.org/10.3390/min13040490>

Academic Editor: Elsabe Kearsley

Received: 7 February 2023

Revised: 22 March 2023

Accepted: 28 March 2023

Published: 30 March 2023



Copyright: © 2023 by the authors. Licensee MDPI, Basel, Switzerland. This article is an open access article distributed under the terms and conditions of the Creative Commons Attribution (CC BY) license (<https://creativecommons.org/licenses/by/4.0/>).

1. Introduction

In the modern world, an important challenge facing humankind is its consumption of natural resources and the related problem of environmental pollution. With an increasing world population and higher living standards, energy demands are continuously increasing, with approximately 35% of electricity produced by burning coal [1]. This high proportion of electricity produced by coal-burning power stations constitutes the largest single source of CO₂ emission and also produces a large amount of solid waste in the form of coal combustion by-products [2–4]. These combustion by-products can be categorized as fly ash, bottom ash, and flue gas de-sulfurization materials. Very often, fly ash or a mixture of fly ash and bottom ash is removed from the power stations by water treatment and stored in ponds or lagoons. After some time when the ponds are full of ash, the top layer may be mixed with soil and revegetated, becoming so-called pond ashes or land-filled ashes [5,6], which serve no useful purpose. According to the latest research on the utilization of

coal combustion by-products, over 50% of ash is used in the production of building and construction materials as additives to concrete and road pavements [7]. The addition of fly ash to a concrete mixture is based on its chemical composition (its pozzolanic or hydraulic nature) and its morphological features which are responsible for the “ball bearing effect” which results in a reduced water demand and improves the strength of the concrete. The addition of fly ash to concrete has the advantage of reducing the cement content, while at the same time decreasing the amount of fly ash going to waste and improving the durability of the resulting concrete. It has been estimated that the worldwide production of concrete is 30 billion tons [8], and the production of OPC (ordinary Portland cement) is estimated to be responsible for 8%–9% of global anthropogenic CO₂ [8]. Thus, the use of fly ash as a partial substitute for OPC in concrete has the two advantages of decreasing the amount of cement and decreasing the amount of fly ash dumped as landfill. However, another alternative is to completely eliminate the use of OPC in concrete by using the fly ash to produce geopolymers, which are materials that have less environmental impact than OPC [9]. Geopolymers are three-dimensional cross-linked inorganic polymers that are produced through the dissolution of amorphous aluminosilicate sources (metakaolin, fly ash) using an alkali metal hydroxide and/or alkali silicate solution [10].

The application of fly ash for geopolymer production has attracted much interest from researchers and fly ash producers around the world because of the potential of these materials to solve modern sustainability issues. There are many publications related to fly-ash-based geopolymers and their applications based on their excellent properties such as their mechanical strength, thermal and acid resistance, low thermal conductivity, etc. A recent review paper describes the variation in and predictability of the splitting tensile strength, flexural strength, and elastic modulus of geopolymer concrete, and especially its compressive strength which opens up the possibility of many more applications of high-strength geopolymers [11].

The principal geopolymerization process includes dissolution–polycondensation reactions in the gel state. Thus, the most important reaction is the dissolution of the aluminate or silicate species in the alkaline solution. In order to increase the dissolution rate of the aluminosilicate into alkaline liquids, various methods such as mechanical, chemical, and thermal activation have been used [12]. Of these activation methods, mechanical activation by milling is attractive due to its ease and simplicity. Mechanical milling induces physical changes such as stress and strain in both the crystalline reactant and the glass particles, resulting in the increased surface area and reactivity of the powders [12–14]. Fly ash can be activated by various types of milling, including attrition, vibration, and tumble milling, etc. The influence of mechanical activation on the physico-chemical properties of the fly ash reactant, and consequently the properties of the geopolymer product cured at room or moderate temperature, has been studied, and improved geopolymerization has been reported in the milled reactants [15–17].

Other aspects which must be considered if mechanical activation is to be used to improve geopolymerization are the economic and environmental benefits, which should not compromise the product quality [7].

Economic benefits generally come from the good mechanical properties of the more expensive geopolymer concretes or pastes; these benefits must balance the energy consumed for milling. In practical terms, the milling needs to be carried out with the lowest possible energy consumption that gives the best outcome, as judged by the particle size reduction and crystalline structure distortion. The same mill may be operated either under continuous dynamic or batch static conditions. In our previous research, we have observed a more beneficial effect of batch attrition milling of fly ash in comparison with vibration milling [18]. From a practical point of view, milling the fly ash in a continuous regime is preferable, as it allows the mechanically activated fly ash to be produced with high productivity and without interruption.

By comparison, batch dry grinding is employed when the material requires longer residence time in the mill (30 min or more), and the prime consideration is to secure the finest possible particle size with a tighter size distribution.

Continuous dry grinding has the following advantages [19]:

1. Production of a large quantity of product.
2. No overheating of the powders inside the milling chamber, especially important for temperature-sensitive materials.
3. Less chance of the ground powders building up against the grinding chamber wall due to the constant movement of the powder.

This paper reports our latest research on continuous dry milling, comparing the applicability of attrition and batch ball milling to the practical production of fly-ash-based geopolymers.

2. Experimental Section

2.1. Fly Ash Milling Procedure

The starting material for these experiments was fly ash from the 4th thermal power station of Ulaanbaatar city. Attrition milling was carried out in an HAS-1 mill (Union Process Co., Akron, OH, USA). This mill had a 5 L grinding volume with 3 kg of 1 cm dia. hardened steel grinding balls, and 0.64 kg of the fly ash was continuously milled for 20 min at an attrition speed of 700 rpm.

Ball milling was carried out in an AXB-100S-5H ball mill (Eishin Co., Ltd., Tokyo, Japan) using the steel balls in the specially designed, hardened, stainless steel sample container as supplied with this equipment. The weight of each 1 cm dia. grinding ball was 4.16 g, and a total of 3.36 kg of balls was used. The ratio of balls to fly ash was 40:1. Milling was carried out for 30 min and 1 h.

2.2. Preparation of the Alkali-Activated Materials

Geopolymers were prepared from ball-milled, attrition-milled, and, for comparison, unmilled fly ash. We activated 300 g of the different fly ash samples with 100 mL of 8 M NaOH solution. Because the attrition-milled fly ash settled quicker than the other fly ash samples, 104 mL NaOH was used with this sample to maintain a working consistency. The fly ash and alkaline liquid mixtures were hand-mixed with a spatula to a uniform consistency. The consistency of all the mixtures was almost identical after 3 min of hand mixing. The activated pastes of uniform consistency were poured into cubic iron molds with 20 mm edges. After wrapping in a plastic bag, they were cured in an oven at 40 °C for 3 days, then removed from the oven, unwrapped, and stored at ambient temperature. The compressive strengths of the samples were measured after 7, 14, and 28 days after preparation.

3. Characterization

XRF analysis of the fly ash was carried out using a wavelength-dispersive X-ray fluorescence spectrometer (PANalytical Axios). The raw and milled fly ash starting materials were characterized by powder XRD, FTIR, SEM, Blaine surface area, and particle size distribution by a sieve analysis. The alkali-activated materials were characterized by powder X-ray diffraction (XRD), Fourier transform infrared spectrometry (FTIR), compressive strength measurements, scanning electron microscopy (SEM,) and bulk density measurements.

X-ray diffraction (XRD) of the starting materials and geopolymers was carried out using a BRUKER D8 Endeavor X-ray diffractometer with cobalt radiation ($C_{\alpha 1} = 1.7890 \text{ \AA}$) in the angular interval $2\theta = 6^\circ\text{--}80^\circ$. The mineral phase identification was performed using X'Pert High Score Plus v3.0 software. Blaine surface area was determined by the air permeability test (PSH-2), as used for characterization of the fineness of a cement powder. The reported Blaine surface area was the average of two measurements which agreed with negligible difference. The particle size distributions were determined by sieve analysis. The compressive strengths of the geopolymer samples were determined after each designated curing time using a UTM-50 instrument. For compressive strength measurements, we used

at least 4 samples, and reported values are the average results of 4 measurements. The crushed geopolymer fragments were used for the XRD, SEM, and FTIR measurements.

The FTIR spectra of the raw and milled fly ashes and their respective geopolymers were determined on samples suspended in KBr discs using a Shimadzu FTIR 8200PC spectrometer. The morphology of the fly ash samples and the microstructures of the geopolymers were characterized by electron microscopy of the surface of the fly ash powders embedded in resin and ground on a SiC disc, and then polished with 9, 3, and 1 μm diamond pastes. The electron micrographs of the polished specimens were obtained using a TESCAN TIMA3 microscope. The bulk densities were determined as the ratio of the weight and the geometrical volume of the samples measured by digital caliper. The densities were taken as the average of 2 measurements.

In this study, the raw fly ashes, the ashes ball-milled for 30 and 60 min, and the attrition-milled samples are denoted as Raw_FA, 30_Bm_FA, 60_Bm_FA, and Am_FA, and the corresponding geopolymer samples are denoted as GP_Raw_FA_7D, 28D; GP_Bm30m_FA_7D, 28D; GP_Bm60m_FA_7D, 28D; and GP_Am_FA_7D, 28D.

4. Results and Discussion

4.1. Influence of Fly Ash Milling on Its Physico-Chemical Properties

The chemical composition of the raw fly ash (wt.%) is: 47.82 SiO₂, 14.87 Al₂O₃, 11.9 Fe₂O₃, 16.03 CaO, 3.16 MgO, 1.31 SO₃, 0.72 TiO₂, 0.91 K₂O, 0.24 Na₂O, 0.41 Mn₃O₄, 0.08 P₂O₅, 0.06 BaO, 1.39 LOI. The raw fly ash contains magnetite (Fe₃O₄), mullite (3Al₂O₃·2SiO₂), quartz (SiO₂), hematite (Fe₂O₃), and anorthite (CaO·Al₂O₃·2SiO₂). Based on the content of calcium and other major oxides, the ASTM classification of this fly ash is C-class. The effect of ball milling and attrition milling on the Blaine surface area and granulometric characteristics of the fly ash is shown in Table 1. Although attrition milling was carried out in continuous mode, it results in the highest Blaine surface area. The fly ash ball-milled for 60 min has a lower Blaine surface area than that milled for 30 min, which remains unchanged. This may be explained by agglomeration in the fly ash ball-milled as a discrete batch in contrast with the continuously milled fly ash.

Table 1. Change in the Blaine surface area and particle size of the ball-milled and attrition-milled fly ashes.

Sample	Surface Area (cm ² /g)	<25 μm , %	<38 μm , %	<43 μm , %	>43 μm , %
Raw_FA	4017	16.36	25.54	44.81	45.2
30_Bm_FA	3999	18.37	51.75	65.04	29.03
60_Bm_FA	3912	10.78	53.72	68.19	26.97
Am_FA	5545	11	60.57	70.92	27.75

Granulometric characterization of the fly ashes treated by ball or attrition milling suggests that more prolonged milling did not cause a decrease in the number of fine particles. The greatest reduction occurs in the 25–43 μm range, while the raw fly ash contains the finest particles in the range of 43 and 75 μm . The data also show that milling decreases the particle size to less than 25 μm after 60 min ball milling and attrition milling. This suggests that some agglomeration of the fine particles has occurred, consistent with the results of the Blaine surface area measurements of the sample ball-milled for 60 min, but seems to be contrary to the attrition milling which may have introduced a degree of porosity in the milled fly ash in the 25–38 μm range. The granulometric characterization of the milled fly ashes suggests that milling produces a negligible reduction in particle size, especially in the size range below 25 μm . The greatest degree of particle size reduction occurs in particles larger than 25 μm . The most significant degree of particle size reduction (up to 38 μm) occurs in the attrition-milled fly ash, probably within the glass phase.

The XRD patterns (Figure 1) show the presence of quartz, magnetite, hematite, and akermanite phases as the main constituents of the crystalline phases, with minor amounts of mullite and anorthite. In general, there is almost no change in the crystalline phases of the fly ashes after milling. Additionally, no significant change in the relative contents of the crystalline and amorphous contributions of the milled samples and the raw fly ash is apparent by direct superimposition of the diffraction patterns. A relatively large X-ray amorphous contribution between 27 and 45° 2 θ was estimated by integration using a background correction based on data between 5 and 15° 2 θ with a linear extrapolation to 80° 2 θ , showing that this amorphous content remains approximately unchanged. However, this does not rule out the possibility that the main changes introduced by milling occur in the amorphous phases. This would support our view that the increase in surface area of the attrition-milled fly ash is related to the amorphous particles.

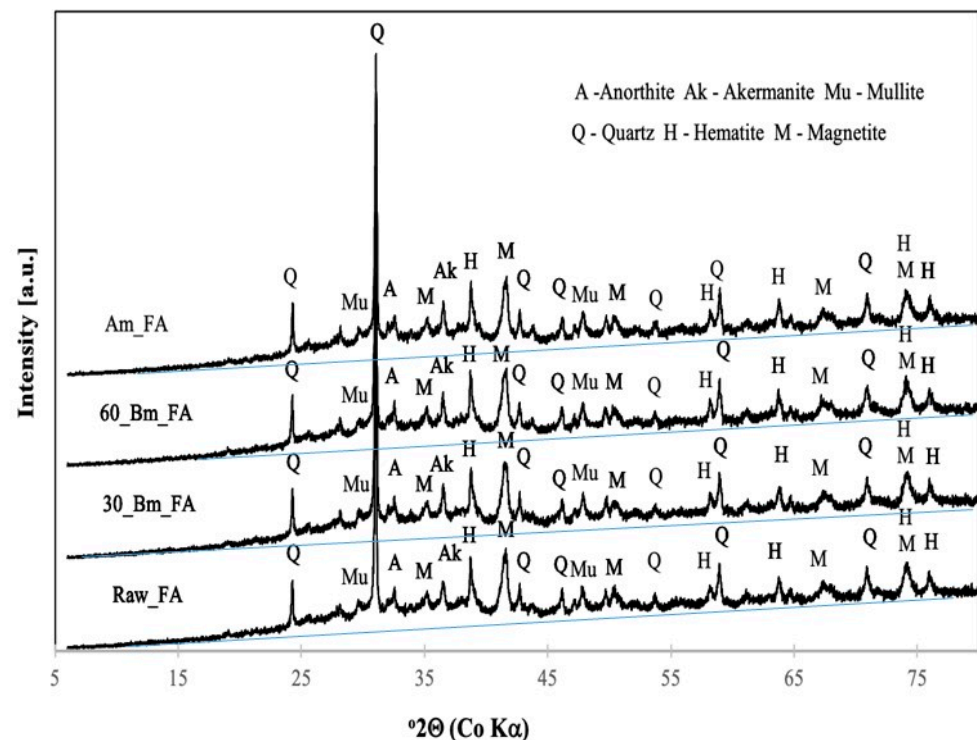


Figure 1. XRD patterns of the raw and milled fly ashes. Thin line shows the linear extrapolation from data between 5 and 15° to 80° for the experimental baseline to provide a better visualization of the amorphous contribution with respect to the crystalline contribution given by the diffraction peaks.

The FTIR spectra (Figure 2) of the milled samples show absorption bands centered at 463–470, 778–796, 1096–1099, and around 3449 cm^{-1} ; these retain a similar shape and position irrespective of the milling treatment. This suggests that milling does not change the bonding state of the raw fly ash. The spectra of the fly ash sample ball milled for 60 min show an increased intensity in the bands of adsorbed water molecules at 1630 (the bending mode) and 3449 cm^{-1} (the OH-stretching modes). The stretching and bending modes of the Si-O bond are shown in Figure 2.

The SEM micrographs of the raw and milled fly ash samples (Figure 3) indicate that there is little difference in the morphology introduced by milling, with spherical particles observed as reported previously [18]. The sample ball-milled for 60 min shows an agglomerated microstructure, consistent with the surface area data (Table 1).

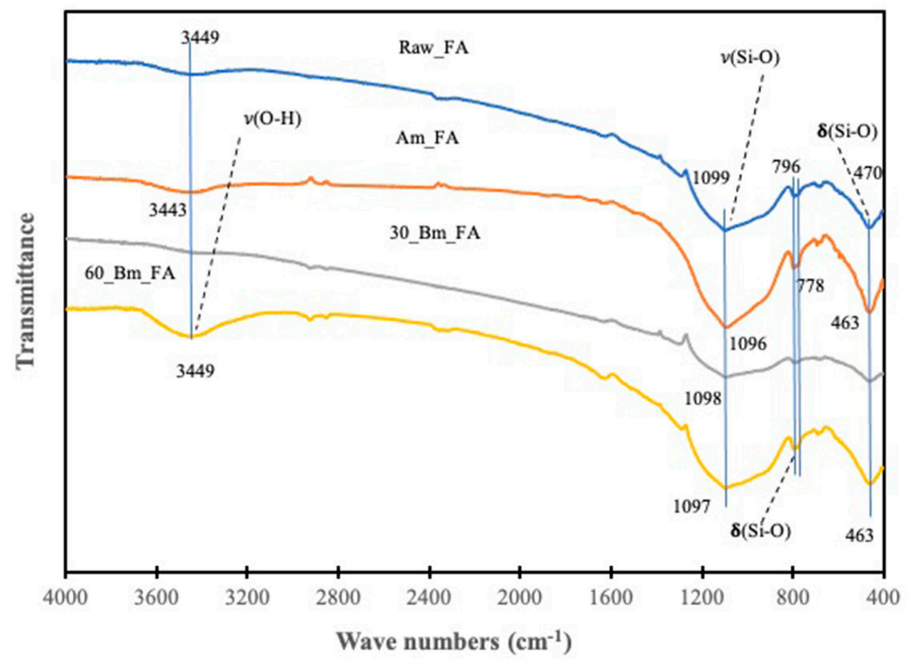


Figure 2. FTIR spectra of the raw and milled fly ashes.

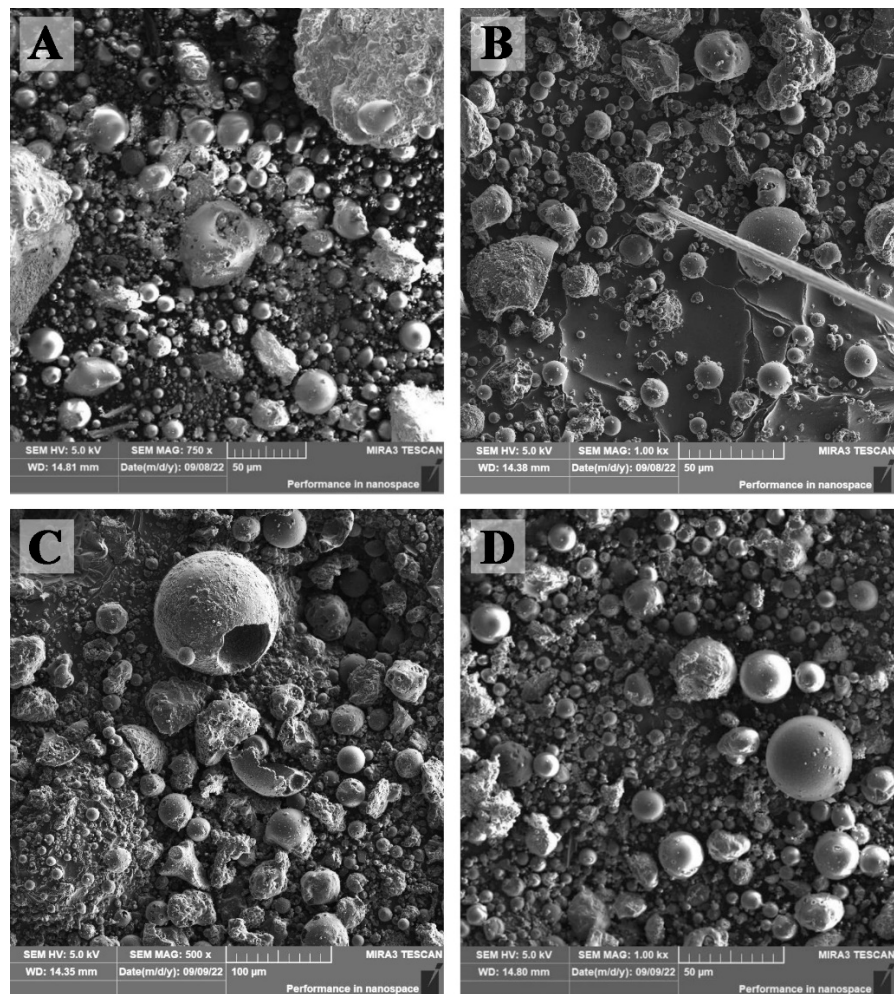


Figure 3. SEM micrographs of the milled and unmilled fly ash. (A) Ball-milled 30 min, (B) ball-milled 60 min, (C) attrition-milled, (D) raw.

4.2. Influence of Milled Fly Ashes on the Properties of Geopolymers

Visual examination of the samples prepared for the compressive strength measurements revealed a brittle glass-like appearance of the geopolymers prepared from the attrition-milled fly ashes. These geopolymers also showed microcracks, and during compressive strength testing, they ruptured noisily, as usually occurs in ceramic-like brittle materials. This may indicate the increased presence of a glass-like gel phase in the attrition-milled geopolymers.

Figure 4a,b show the XRD patterns of the geopolymer pastes cured for 7 and 28 days. The XRD patterns of the cured samples resemble those of the raw and milled fly ash starting materials, with no apparent change in the crystalline components resulting from the alkaline treatment. This suggests that the geopolymer-forming reactions occur principally in the amorphous component of the fly ash, with negligible participation of the crystalline components. In contrast with previous work on geopolymer formation from ash from the fourth thermal power plant of Ulaanbaatar city [20], zeolite formation was not observed in the cured products. This may be related to the low curing temperature of the present samples (40 °C) where the dissolution rate of the fly ash is low. Using the baselines shown in Figure 4, the integration of the total intensity with respect to the diffracted peak intensity indicates that between 37 and 45% of the diffraction patterns is related to the amorphous contribution, i.e., this represents a small change in the amorphous content. On the other hand, a small but significant shift in the scattered intensity from lower 2° theta values (say from 20° to 30°) to higher 2° theta values (30° to 40°) is observed when calculating the difference patterns of the raw and milled samples minus those of the related alkali-activated samples. As a cross check, the difference pattern of the milled pattern does not show this effect. A related but more pronounced observation is discussed below in connection with the FTIR absorption spectra (Figure 5a,b).

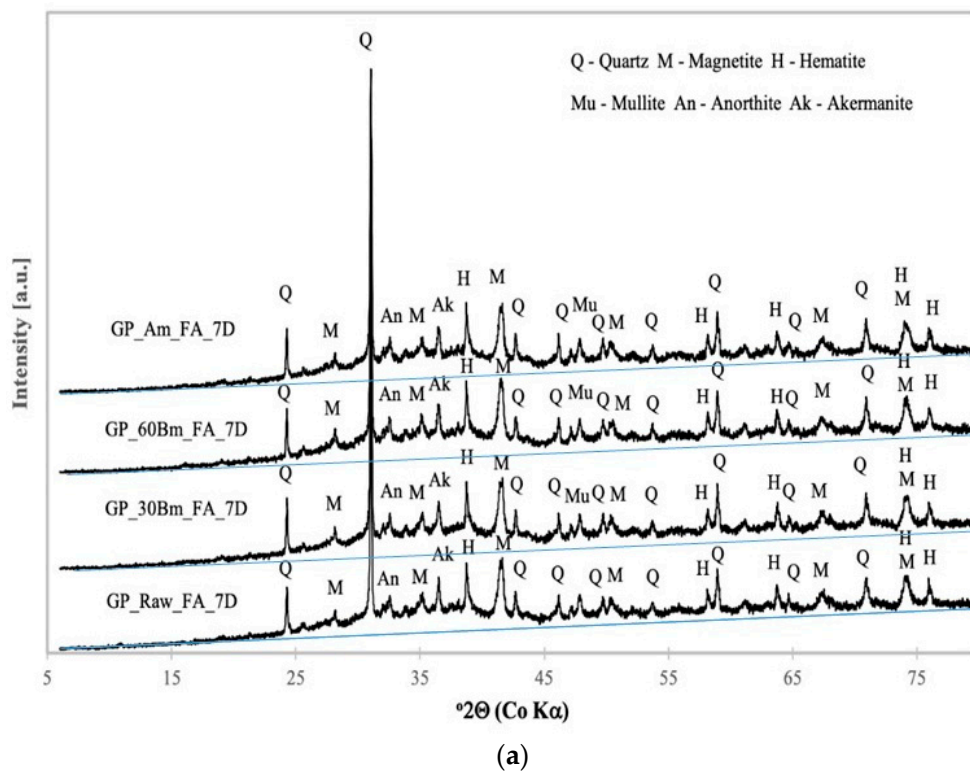


Figure 4. Cont.

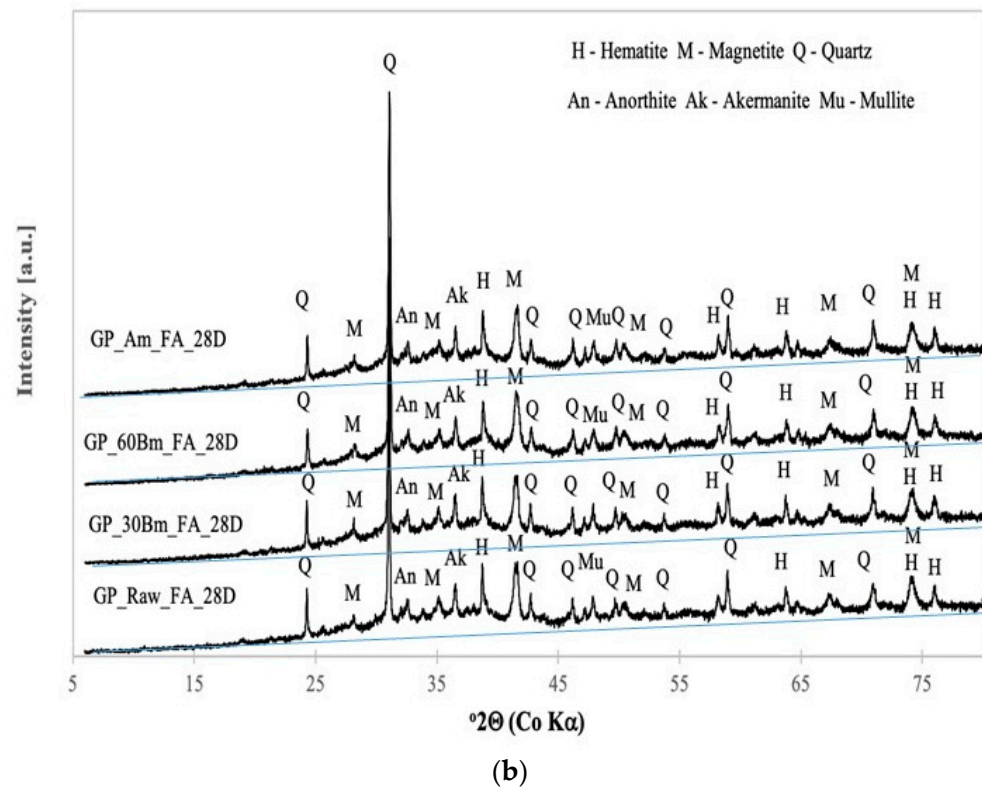
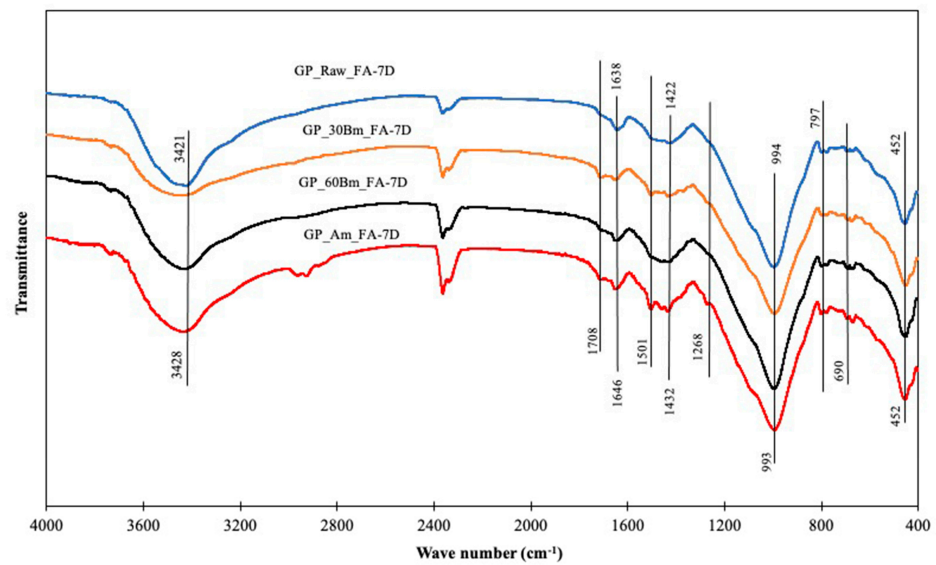


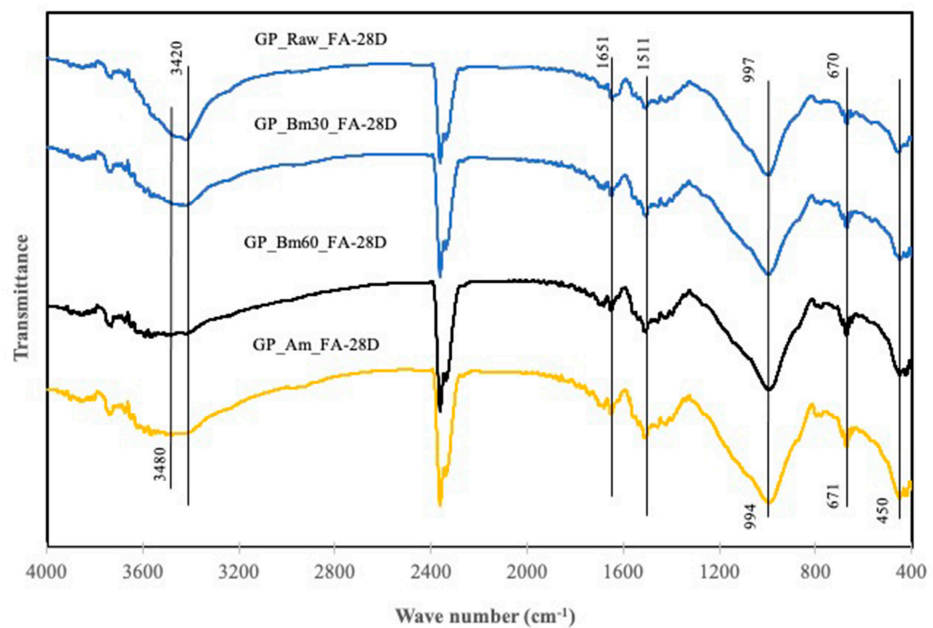
Figure 4. XRD patterns of the geopolymer pastes cured for (a) 7 days and (b) 28 days. Thin lines show a linear extrapolation from data between 5 and 15° to 80° for experimental baseline for better visualization of the amorphous contribution with respect to the crystalline contribution given by the diffraction peaks.

Figure 5a,b show the FTIR spectra of the geopolymer pastes cured for 7 and 28 days. The FTIR spectra contain absorption bands of similar shape and position, which differ significantly from the spectra of the raw and milled fly ash samples (Figure 2). The peak maxima of the main absorption bands of the geopolymer samples are at about 993–998 cm^{-1} and 450–452 cm^{-1} and are lower than those of the fly ash samples by about 100 and 15 cm^{-1} , respectively. There are only slight deviations between the geopolymer samples cured for 7 and 28 days, taking into account the possibility of experimental uncertainties introduced by atmospheric conditions for referencing and sampling (e.g., the effect of the atmospheric CO_2 contribution at 2400 cm^{-1}). However, it is clear that the absorption peaks in the range of 1400–1520 cm^{-1} are due to $(\text{CO}_3)^{2-}$ formed on exposure of the NaOH solution to atmospheric CO_2 . Moreover, the absorption bands at about 3420 and 3480 cm^{-1} and those at 1650 cm^{-1} (in the 28-day sample) and 1638, 1646, and 1708 cm^{-1} (in the 7-day sample) are related to the stretching and bending vibrations of the H_2O molecules, respectively. These H_2O molecules are formed by the polycondensation reactions and become enclosed in the geopolymer network. The concentration of these species is much larger in comparison with the surface-adsorbed H_2O species, as seen in the sample ball-milled for 60 min (Figure 2).

Zhang et al. [21] classified the vibrational bands in the IR spectra into active and inactive bands and suggested that the effect of the dissolution of the Al and Si atoms that participate in the geopolymerization reaction could be seen more easily in the active bands.



(a)



(b)

Figure 5. FTIR diagrams of the raw and milled fly-ash-based geopolymers cured for (a) 7 days and (b) 28 days.

The active bands are defined as those bands enveloped in the density of states of the asymmetric vibrations of the [SiO₄] units. The incorporation of silicate units (Si-O-Al) into siloxo units (Si-O-Si) or cross-linking of the various units in the geopolymerization process is detected in the shift of the density of states peak maximum (DOSPM), which is characterized by the position of the asymmetrical stretching vibration of the maximum of the peak [22]. As an analogy to the shift in the DOSPM observed in aluminosilicate glasses related to the Si/Al ratio and the effect on the DOSPM of geopolymers with and without the addition of Ca cations, an earlier study [22] is also appropriate. In the present study, an interesting observation is that activation with the NaOH solution produces a DOSPM at about 994–997 cm⁻¹ in all cases, compared with the DOSPM at about 1096–1099 cm⁻¹ in raw fly ash and milled samples (Figure 2). The DOSPM of about 994–997 closely agrees

with the DOSPM of CSH-type phases [22]. Since, as shown above, the reaction occurs in the amorphous phase, this indicates that the amorphous CSH is also produced by activation of the fly ash by the NaOH solution. Therefore, the FTIR results suggest that the gel formation mechanism in the fly ash is related to the formation of amorphous aluminosilicate (geopolymer) and CSH (cement) types of products. However, the present experimental observations do not allow the geopolymer and CSH-type products within the binder phase to be distinguished.

SEM micrographs and EDS spectra of the geopolymers based on the raw and milled fly ash are shown in Figures 6–8. The microstructures of the 7- and 28-day specimens kept at ambient temperature are essentially similar. The geopolymer samples consist of partly dissolved and non-dissolved spherical fly ash particles and a newly formed structure which we suggest results from the dissolution of the fly ash constituents. The newly formed structure contains Na, Al, Si, and Ca in a gel-type microstructure that covers the intact fly ash. The 7- and 28-day samples consist of a non-dense, porous microstructure containing some cracks. These results suggest that the dissolution of the fly ash forms a mixture of amorphous or semi-crystalline sodium aluminosilicate (NASH), calcium aluminosilicate (CASH), or calcium silicate hydrate (CSH) type phases. The SEM micrographs (Figure 8) indicate that few changes occur in the samples after 7- and 28-day curing, and changes in the microstructure at longer curing times are negligible. This suggests that geopolymerization is slow and continuous at the ambient temperature of the present experiments. Although the main microstructure change was expected to be crystallization within the amorphous gel, the formation of whiskers or crystals in the microstructure was not observed, even in the 28-day sample. The microstructure of the cured samples is in general agreement with the XRD patterns (Figure 4) and FTIR measurements (Figure 5). Since no crystalline structures were observed by XRD, this suggests that the newly formed structure is amorphous.

Interestingly, although most of the newly formed gel phase contains sulfur, no ettringite-type compounds were observed in the XRD patterns.

Some regions of the attrition-milled 28-day fly ash geopolymer showed the formation of a multi-component system containing various particles together with the crystalline and amorphous structures (Figure 8).

In these samples, the fly ash particles are typical aluminosilicates with a partially dissolved surface layer (A3). Unburned carbon was also detected in the EDS spectrum (A1). An interesting feature of the attrition-milled fly ash geopolymer is the appearance of a polymeric product with a discrete gel-type structure (Figure 7D,D' and Figure 8(A4)). Although these geopolymer products appear similar, they differ in chemical composition. Figure 7D represents the typical geopolymer composition containing Al, Si, Ca, Na, and S atoms, whereas Figure 7D' contains Ca, Na, Si, and S atoms. The latter may represent a non-geopolymer product containing sodium silicate NS and calcium silicate hydrate CSH. The XRD, FTIR, and SEM-EDS analyses suggest the formation of amorphous geopolymer and calcium silicate phases, regardless of the milling conditions in all the fly-ash-based geopolymer samples, together with sodium silicate and calcium silicate in the attrition-milled fly-ash-based sample.

The results of the compressive strength (CS) and bulk density (BD) measurements of the geopolymers are shown as bar diagrams in Figures 9 and 10, respectively. The highest CS value (Figure 9) at all curing times except 14 days is found in the attrition-milled geopolymers, whereas the next highest CS value for the overall samples is found in the geopolymer sample formed from fly ash ball-milled for 30 min, although the values for these samples are in agreement within the limits of error of these measurements (Figure 9). The attrition-milled samples show the highest values of bulk density at all curing times, followed by the samples ball-milled for 30 min (Figure 10).

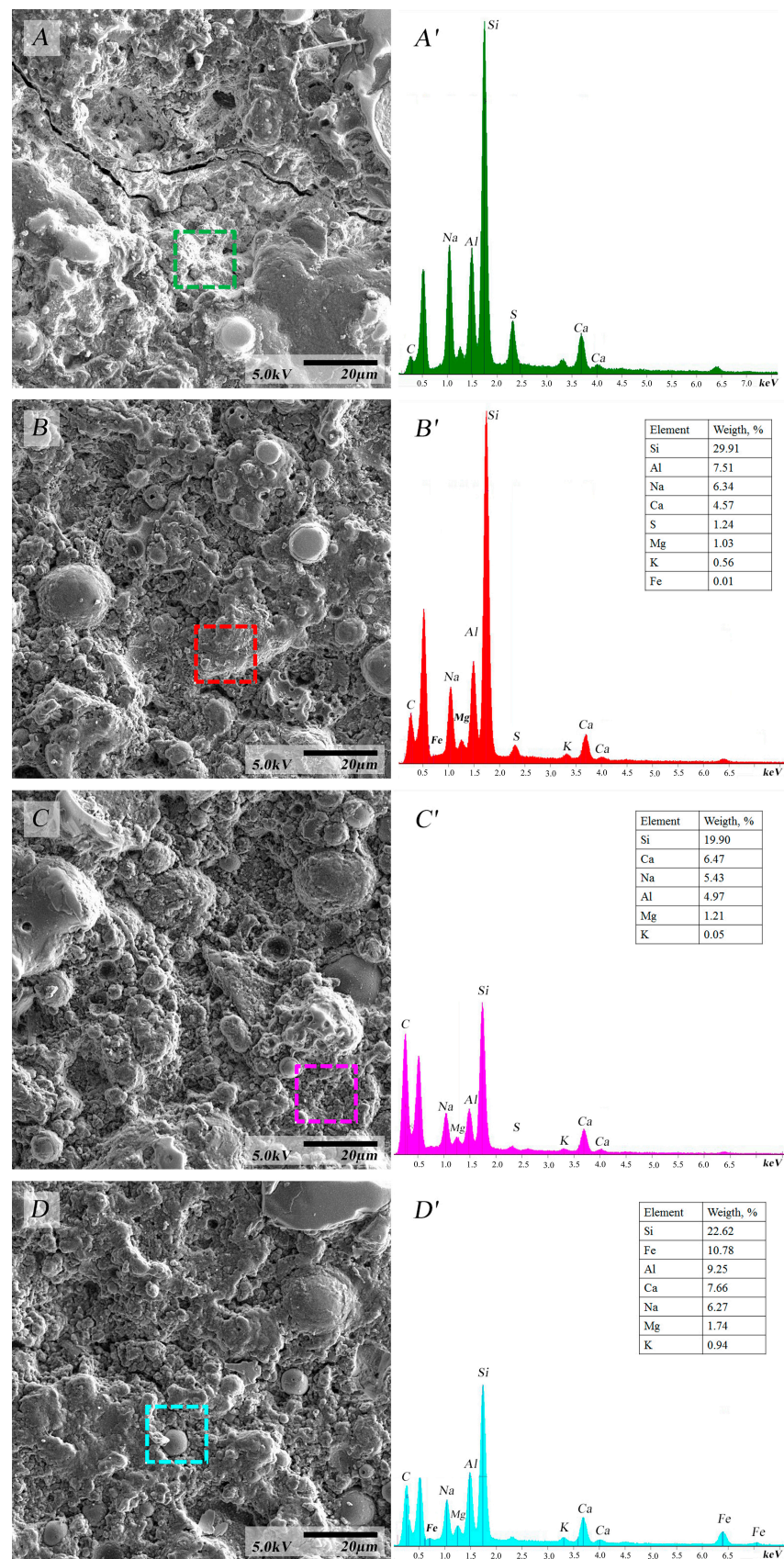


Figure 6. SEM micrographs and the corresponding EDS spectra of the raw and milled fly-ash-based geopolymers after 7 days of curing. (A,A') Raw. (B,B') Ball-milled 30 min. (C,C') Ball-milled 60 min. (D,D') Attrition-milled.

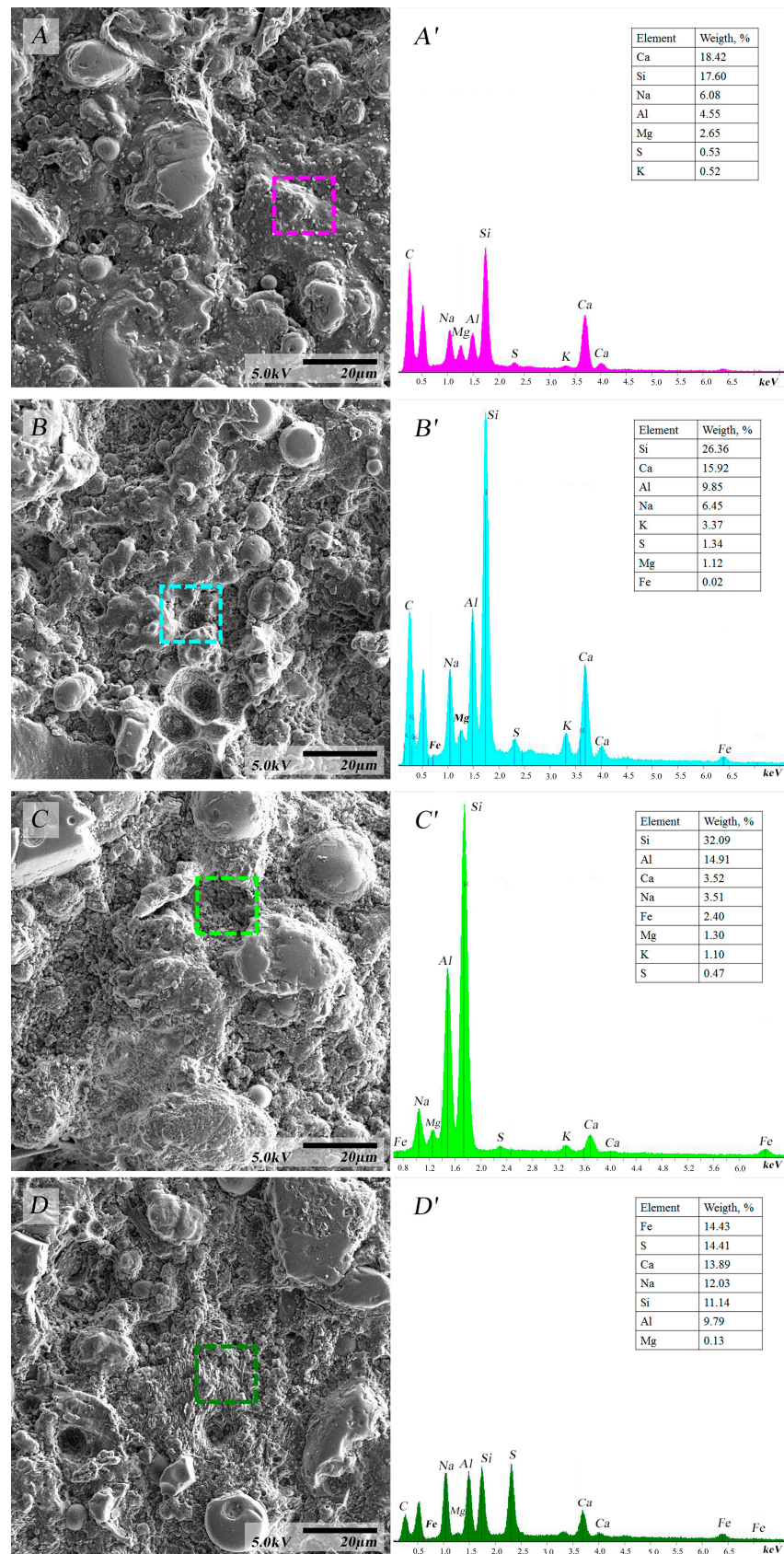


Figure 7. SEM micrographs and the corresponding EDS spectra of the raw and milled fly-ash-based geopolymers after 28 days of curing. (A,A') Raw. (B,B') Ball-milled 30 min. (C,C') Ball-milled 60 min. (D,D') Attrition-milled.

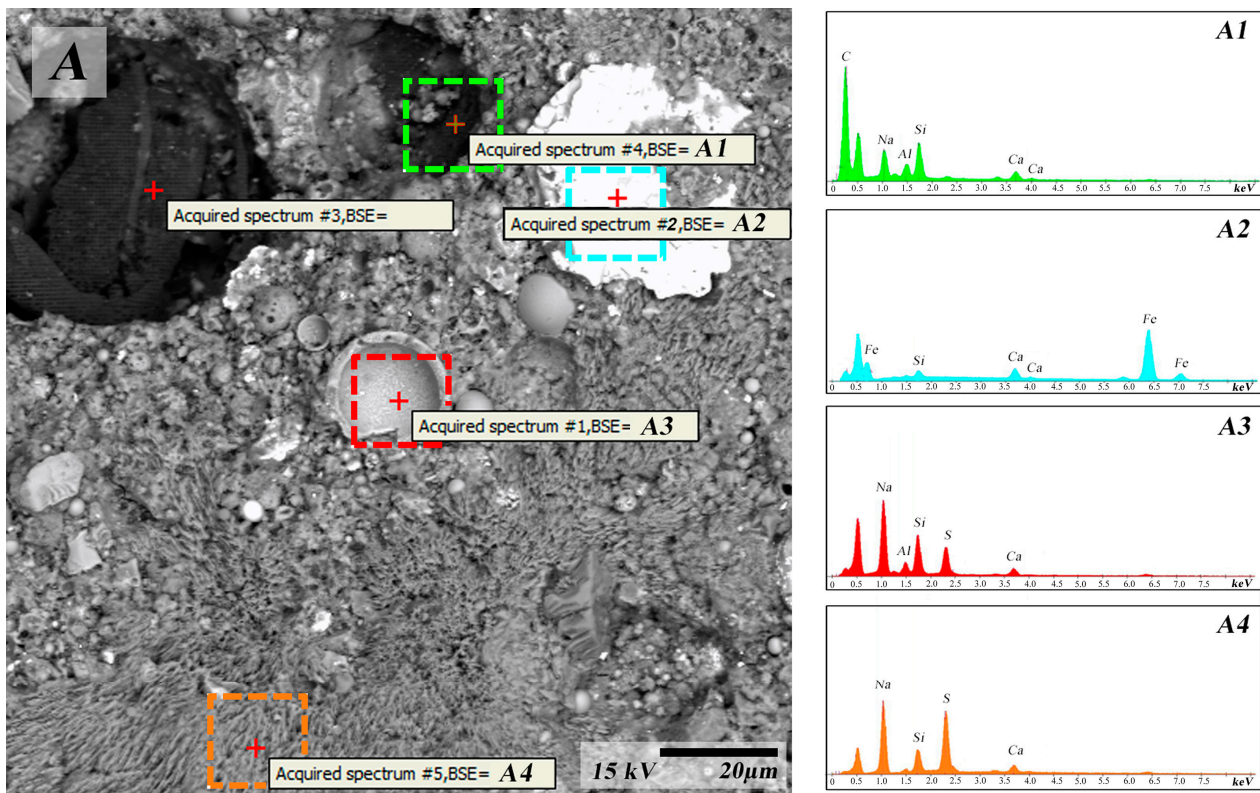


Figure 8. Selected SEM micrographs and EDS spectra of the 28-day attrition-milled fly-ash-based geopolymers.

These results suggest that the different milling processes induce differences in the geopolymerization process, resulting in the formation of different networks or differing degrees of inhomogeneity in the network structure, with the greatest improvement in the mechanical properties secured by attrition milling.

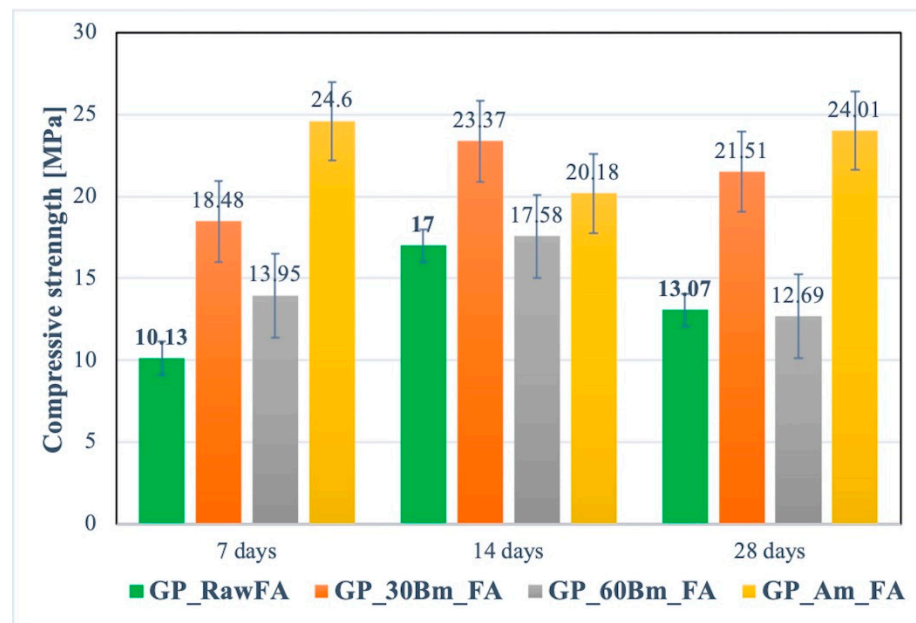


Figure 9. Compressive strengths of the various geopolymers. Error bars represent the standard deviation of a data.

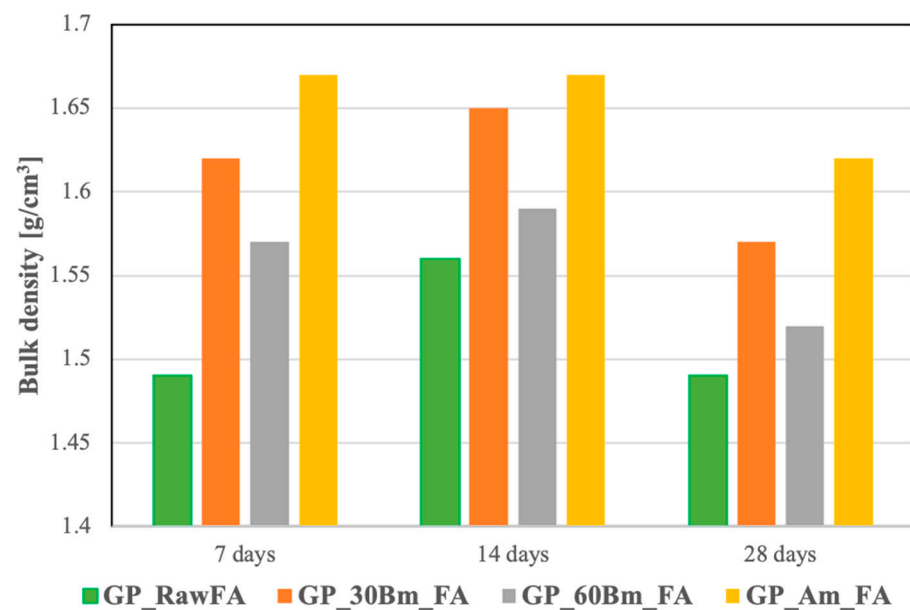


Figure 10. Bulk densities of the various geopolymers.

Figures 9 and 10 show that in general the compressive strengths correlate with the bulk densities of the geopolymers. We also suggest that the principal influence on geopolymerization is the granulometry of the milled fly ash rather than the method of mechanical amorphization. Thus, it is likely that the solubility and dissolution reactions in the milled fly ashes depend on their mineralogical composition and granulometry. We also suggest that the milling process promotes the pozzolanic reaction responsible for the formation of the CSH gel phase, as usually occurs in mechanically activated fly-ash-containing binder systems [23].

The attrition-milled fly ash exhibits a greater degree of dissolution than does the ball-milled fly ash. One possible explanation is related to the aspect of the preparation procedure, namely, curing at the relatively low temperature of 40 °C for 68 h. This low curing temperature was chosen to reduce the processing energy consumption. In our previous research, we used a curing temperature of 70 °C [18,20]. The geopolymerization process consists of the following steps: dissolution, monomer formation, polycondensation, and hardening. In this sequence, the dissolution of the amorphous aluminosilicate sources occurs from the surface and moves preferentially along weakened zones into the interior. For this reason, finer particles dissolve preferentially and at a faster rate at higher temperatures. In the present study, the curing temperature of 40 °C was not sufficiently high for complete geopolymerization, as was achieved at 70 °C. We suggest that this is the explanation for the relatively small change in the compressive strength of the samples cured for 7 and 28 days. Geopolymerization was essentially complete within 7 days in the milled fly ash pastes, and further increases in the curing time did not increase the reaction rate at 40 °C. Another possible explanation for the change in the compressive strength of the sample cured for 28 days is related to moisture loss from the samples maintained at ambient temperature after curing at 40 °C. It is possible that the moisture loss from the samples held for longer times at ambient temperatures after curing does not allow the geopolymerization reaction to proceed further.

The higher compressive strength of the attrition-milled fly ash geopolymers is consistent with the smaller particle size resulting from continuous milling. In our previous research [18], we used batch attrition milling of the same fly ash for geopolymerization and compared it with the vibration-milled fly ashes. The 7-day compressive strengths of the raw, batch-attrition-milled, and vibration-milled fly ashes were 21.3 MPa, 60.56 MPa, and 49.53 MPa, respectively. These compressive strengths of the same raw and batch-milled fly ashes were 2–2.4 times higher than those obtained in the present research. The main reason

for this discrepancy is probably related to the lower curing temperature of the present study. Kato et al. have reported similar results in which mechanochemical treatment of their fly ash was correlated with changes in its surface morphology and crystal structure and its behavior upon alkali activation [24]. These authors suggested that the change in the particle morphology after short-term mechanical activation was the dominant effect upon alkali leaching, whereas amorphization was the dominant effect upon alkali leaching in fly ash milled for a longer time [24]. The same behavior was also reported for the ball-milled and batch-attrition-milled fly-ash-based geopolymer pastes [18]. In other words, regardless of the milling regime, attrition milling is more beneficial for fly ash activation than ball milling. Since various other studies have carried out the preparation of geopolymer pastes at different curing temperatures of fly ash activated by continuous dynamic and batch static attrition milling methods, a direct comparison of the properties of continuously milled and batch-milled fly ash geopolymers cannot be made. However, attrition-milled fly ash required higher curing temperatures to accelerate geopolymer formation. Although direct evidence is lacking, the mineralogical composition of the different fly ash fractions appears to exert a substantial influence on geopolymerization. Based on the fly ash fraction content, it may be speculated that the mineralogical composition of the milled fly ash within the <43 μm size range is the determining factor in the formation of the binder phase.

5. Conclusions

The effect of the production regime and the milling technique on the formation of fly-ash-based geopolymers, as reflected in their compressive strengths, has been studied, with the following conclusions:

Continuous attrition milling and static ball milling both cause structural distortions in the fly ash, but the chemical bonding state of both the ball-milled and attrition-milled fly ash is virtually unchanged. However, the main difference in the properties of the milled fly ash was a change in its surface area and granulometry. Attrition milling resulted in an increase in surface area of more than 30%, from 4017 cm^2/g to 5545 cm^2/g , whereas a reduction in surface area from 3999 cm^2/g and 3912 cm^2/g was found in fly ash ball-milled for 30 and 60 min. Continuous attrition milling produces a beneficial size reduction, together with an improvement of the resulting geopolymers. Static ball milling produces an agglomerated microstructure which is not beneficial for geopolymerization. The highest compressive strength of the attrition-milled fly ash geopolymers was 24.6 MPa, whereas geopolymers based on unmilled fly ash and fly ash ball-milled for 30 and 60 min show the highest compressive strengths (17, 23.37 and 17.58 MPa, respectively). Curing temperatures should be higher than 40 $^\circ\text{C}$, as used in the present study, in order to complete the geopolymerization reaction within the binder phase. The mineralogical composition and content of the milled fly ash fractions exert a substantial influence on binder phase formation. Milling accelerates not only the geopolymer-type reaction to form the aluminosilicate network but also the pozzolanic reaction in the fly ash to form a CSH gel phase. Evaluation of the DOSPM (density of states peak maximum) in the infrared absorption leads to the conclusion that both an amorphous CSH-type network and sodium silicate are formed by the reaction of NaOH solution with the fly ash.

Author Contributions: Conceptualization, J.T. and C.H.R.; methodology, J.T.; validation, B.D., U.R., E.O. and D.E.; formal analysis, B.D., E.O. and D.E.; investigation, B.D., U.R. and S.D.; resources, T.T.-A.; data curation, C.H.R. and T.T.-A.; writing—original draft preparation, J.T., writing—review and editing, C.H.R. and K.J.D.M.; supervision K.J.D.M.; project administration, J.T. and C.H.R. All authors have read and agreed to the published version of the manuscript.

Funding: The authors wish to thank the Alexander von Humboldt Foundation for the Digital Cooperation Fellowship and a further grant for two months supporting the stay of JT at LUH under which the present research was carried out.

Data Availability Statement: The data presented in this study are available on request from the corresponding author.

Conflicts of Interest: The authors declare no conflict of interest.

References

1. IEA. Data Statistics. Available online: www.iea.org/statistics/ (accessed on 10 September 2022).
2. Blissett, R.S.; Rowson, N.A. A review of the multi-component utilization of coal fly ash. *Fuel* **2012**, *97*, 1–23. [CrossRef]
3. Asokan, P.; Saxena, M.; Asolekar, S.R. Coal combustion residues—Environmental Implications and recycling potentials. *Res. Conserv. Recycl.* **2005**, *43*, 239–262. [CrossRef]
4. Ahmaruzzaman, M. A review on the utilization of fly ash. *Prog. Ener. Combust. Sci.* **2010**, *36*, 327–363. [CrossRef]
5. Temuujin, J.; Minjigmaa, A.; Bayarzul, U.; Kim, D.S.; Lee, S.H.; Lee, H.J.; Ruescher, C.H.; MacKenzie, K.J.D. Properties of geopolymers prepared from milled pond ash. *Mater. De Construcción* **2017**, *67*, e134. [CrossRef]
6. Mucsi, G.; Kumar, S.; Csoke, B.; Kumar, R.; Molnar, Z.; Racz, A.; Madai, F.; Debreczeni, A. Control of geopolymer properties by grinding of land filled fly ash. *Int. J. Min. Proc.* **2015**, *143*, 50–58. [CrossRef]
7. Temuujin, J.; Surenjav, E.; Ruescher, C.H.; Vahlbruch, J. Review Processing and uses of fly ash addressing radioactivity (critical review). *Chemosphere* **2019**, *216*, 866–882. [CrossRef] [PubMed]
8. Monteiro, P.; Miller, S.; Horvath, A. Towards sustainable concrete. *Nat. Mater.* **2017**, *16*, 698–699. [CrossRef]
9. Provis, J.L. Geopolymers and other alkali activated materials: Why, how, and what? *Mater. Struct.* **2014**, *47*, 11–25. [CrossRef]
10. Lemounga, P.N.; MacKenzie, K.J.D.; Melo, U.F.C. Synthesis and thermal properties of inorganic polymers (geopolymers) for structural and refractory applications from volcanic ash. *Ceram. Int.* **2011**, *37*, 3011–3018. [CrossRef]
11. Mohammed, A.A.; Ahmed, H.U.; Mosavi, A. A Survey of Mechanical Properties of Geopolymer Concrete: A Comprehensive Review and Data Analysis. *Materials* **2021**, *14*, 4690. [CrossRef]
12. Ranjbar, N.; Kuenzel, C.; Spangenberg, J.; Mehrali, M. Hardening evolution of geopolymers from setting to equilibrium: A review. *Cem. Concr. Compos.* **2020**, *114*, 103729. [CrossRef]
13. Kumar, A.; Kumar, R.; Alex, T.C.; Bandopadhyay, A.; Melhotra, S.P. Influence of reactivity of fly ash on geopolymerisation. *Adv. Appl. Cer.* **2007**, *106*, 120–127. [CrossRef]
14. Erdemoglu, M.; Balaz, P. An Overview of surface analysis techniques for characterization of mechanically activated minerals. *Min. Proc. Extract. Metall. Rev.* **2012**, *33*, 65–88. [CrossRef]
15. Temuujin, J.; Williams, R.; Van Riessen, A. Effect of mechanical activation of fly ash on the properties of geopolymer cured at ambient temperature. *J. Mat. Process Technol.* **2009**, *209*, 5276–5280. [CrossRef]
16. Kumar, S.; Kumar, R.; Mehrotra, S.P. Geopolymers, fly ash reactivity and mechanical activation. In Proceedings of the IN-COME2008 Conference, Frontiers in Mechanochemistry and Mechanical Alloying, Jamshedpur, India, 1–4 December 2008; National Metallurgical Laboratory: Jamshedpur, India, 2011; pp. 320–323.
17. Kumar, S.; Kumar, R. Mechanical activation of fly ash, Effect on reaction, structure and properties of resulting geopolymer. *Ceram. Int.* **2011**, *37*, 533–541. [CrossRef]
18. Chu, Y.S.; Davaabal, B.; Kim, D.S.; Kim, S.K.; Ruescher, C.; Temuujin, J. Reactivity of fly ashes milled in different milling devices. *Rev. Adv. Mater. Sci.* **2019**, *58*, 179–188. [CrossRef]
19. Just, A.; Yang, M. *Attrition Dry Milling in Continuous and Batch Modes*; Union Process Inc.: Akron, OH, USA, 2019. Available online: <https://unionprocess.com/wp-content/uploads/2021/02/Attrition-Dry-Milling-In-Continuous-And-Batch-Modes.pdf> (accessed on 30 September 2022).
20. Temuujin, J.; Minjigmaa, A.; Davaabal, B.; Bayarzul, U.; Ankhtuya, A.; Jadambaa, T.; MacKenzie, K.J.D. Utilization of radioactive high-calcium Mongolian flyash for the preparation of alkali-activated geopolymers for safe use as construction materials. *Ceram. Int.* **2014**, *40*, 16475–16483. [CrossRef]
21. Zhang, Z.; Wang, H.; Provis, J. Quantitative study of the reactivity of fly ash in geopolymerization by FTIR. *J. Sustain. Cem.-Based Mat.* **2012**, *1*, 154–166. [CrossRef]
22. Rüscher, C.H.; Mielcarek, E.M.; Wongpa, J.; Jaturapitakkul, C.; Jirasit, F.; Lohaus, L. Silicate, aluminosilicate and calciumsilicate gels for building materials: Chemical and mechanical properties during ageing. *Eur. J. Miner.* **2011**, *23*, 111–124. [CrossRef]
23. Temuujin, J.; Rüscher, C.H. Microstructural and thermal characterization of concretes prepared with the addition of raw and milled fly ashes. *J. Mat. Res. Technol.* **2022**, *20*, 1726–1735. [CrossRef]
24. Kato, K.; Xin, Y.; Hitomi, T.; Shirai, T. Surface modification of fly ash by mechano-chemical treatment. *Cer. Int.* **2019**, *45*, 849–853. [CrossRef]

Disclaimer/Publisher’s Note: The statements, opinions and data contained in all publications are solely those of the individual author(s) and contributor(s) and not of MDPI and/or the editor(s). MDPI and/or the editor(s) disclaim responsibility for any injury to people or property resulting from any ideas, methods, instructions or products referred to in the content.